HHS Public Access

Author manuscript

Curr Biol. Author manuscript; available in PMC 2017 February 22.

Published in final edited form as:

Curr Biol. 2016 February 22; 26(4): 542–549. doi:10.1016/j.cub.2015.12.055.

A Sawtooth Pattern of Cadherin 2 Stability Mechanically Regulates Somite Morphogenesis

Patrick McMillen[1], **Veena Chatti**[1], **Dörthe Jülich**[1], and **Scott A. Holley**[1,*]

[1]Department of Molecular, Cellular and Developmental Biology, Yale University, New Haven, CT 06520, USA

SUMMARY

Differential cadherin (Cdh) expression is a classical mechanism for in vitro cell sorting [1]. Studies have explored the roles of differential Cdh levels in cell aggregates and during vertebrate gastrulation, but the role of differential Cdh activity in forming in vivo tissue boundaries and boundary extracellular matrix (ECM) is unclear [2–6]. Here, we examine the interactions between cell-cell and cell-ECM adhesion during somitogenesis, the formation of the segmented embryonic precursors of the vertebral column and musculature. We identify a sawtooth pattern of stable Cdh2 adhesions in which there is a posterior-to-anterior gradient of stable Cdh2 within each somite, while there is a step-like drop in stable Cdh2 along the somite boundary. Moreover, we find that the posterior somite boundary cells with high levels of stable Cdh2 have the most columnar morphology. Cdh2 is required for maximal cell aspect ratio and thus full epithelialization of the posterior somite. Loss-of-function analysis also indicates that Cdh2 acts with the fibronectin (FN) receptor integrin α5 (Itgα5) to promote somite boundary formation. Using genetic mosaics, we demonstrate that differential Cdh2 levels are sufficient to induce boundary formation, Itgα5 activation, and FN matrix assembly in the paraxial mesoderm. Elevated cytoskeletal contractility is sufficient to replace differential Cdh2 levels in genetic mosaics, suggesting that Cdh2 promotes ECM assembly by increasing cytoskeletal and tissue stiffness along the posterior somite boundary. Throughout somitogenesis, Cdh2 promotes ECM assembly along tissue boundaries and inhibits ECM assembly in the tissue mesenchyme.

Graphical Abstract

*Correspondence: scott.holley@yale.edu.

AUTHOR CONTRIBUTIONS

The research project was conceived and designed by P.M., D.J., and S.A.H. Experiments were performed by P.M., V.C., and D.J. Data analyses were carried out by P.M., V.C., D.J., and S.A.H. P.M. and S.A.H. wrote the manuscript.

SUPPLEMENTAL INFORMATION

Supplemental Information includes three figures and Supplemental Experimental Procedures and can be found with this article online at http://dx.doi.org/10.1016/j.cub.2015.12.055.

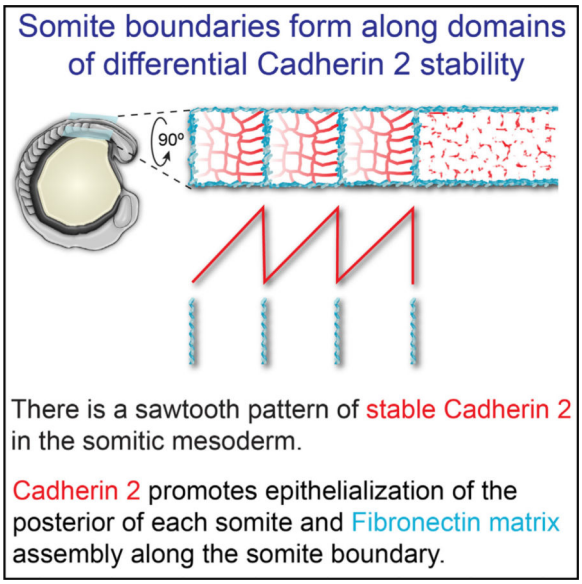

RESULTS AND DISCUSSION

Somite Cell-Shape Changes Correlate with Stable Cadherin Adhesions

Cell morphometrics have been used to infer the mechanical properties of forming tissues in the *Drosophila* wing disc and embryo, and in aggregates derived from zebrafish gastrulae [5, 7–10]. Our morphometric analysis reveals that the posterior boundary cells of nascent somites are more epithelialized than the anterior boundary cells (Figures 1A–1D). The posterior boundary cells are elongated along the anterior-posterior axis and compressed along the medial-lateral axis, suggesting that they are under greater cytoskeletal tension than cells along the anterior somite boundary (Figure 1C). As cadherins are effectors of differential tension, we asked whether differential Cdh2 levels correlate with these shape changes [11]. Importantly, total cadherin levels are not necessarily an accurate indicator of cadherin activity. In both *Drosophila* and *Xenopus*, cells have been shown to contain distinct populations of immobile engaged cadherins and freely diffusing unengaged cadherins [12, 13]. We thus investigated whether the cell-shape changes that we observe along posterior somite boundaries could be explained by differential distribution of stable adherens junctions using a Cdh2 fluorescent timer containing both a fast-folding sfGFP and a slow-folding TagRFP [14].

Examination of total Cdh2 via sfGFP fluorescence reveals relatively uniform Cdh2 distribution throughout the somite, consistent with previous immunohistochemical analyses [15, 16], but a reduction in Cdh2 along the somite boundary [17]. In contrast, stable Cdh2 adhesions as visualized via TagRFP fluorescence display a clear posterior-to-anterior gradient within the nascent somites (Figures 1E and 1G). Given that high levels of stable Cdh2 correlate with the columnar morphology of the posterior somite boundary cells, we asked whether Cdh2 is necessary for this cell morphology. We compared cell aspect ratios in *cdh2*$^{-/-}$ and wild-type sibling embryos and found that Cdh2 is indeed required for maximal elongation of the posterior somite boundary cells (Figures 1F and S1). In contrast, Cdh2 is

not required for the polarized orientation of the posterior boundary cells with respect to the somite boundary (Figure S1).

The serially repeated gradients of stable Cdh2 form a sawtooth pattern that results in a sharp boundary between cells with high stable Cdh2 and cells with low stable Cdh2 along somite boundaries. Meanwhile, the graded transition within the somite precludes sharp contrasts in Cdh2 levels. The differential Cdh2 levels at somite boundaries are reminiscent of cell aggregate experiments in which differential cadherin levels are sufficient to drive cell sorting [4]. Thus, we tested whether differential cadherin levels are sufficient to induce tissue boundary formation in the paraxial mesoderm.

Differential Cdh2 Expression Induces Formation of ECM-Containing Tissue Boundaries

We generated tissue mosaics via blastoderm-stage cell transplantation to recapitulate the sharp difference in Cdh2 levels along somite boundaries using *fss*/*tbx6*$^{-/-}$ embryos, which lack endogenous somite boundaries (Figure 2A). This approach has been used to identify factors that are sufficient to drive morphological boundary formation, including ephrinB2A reverse signaling and differential *itgα5* expression [16, 18, 19]. We generate Cdh2-deficient cells by injecting an antisense morpholino that recapitulates the *cdh2*$^{-/-}$ phenotype (Figure S2) and reduces both total and stable Cdh2 when injected into the Cdh2 timer transgenic (Figure S2) [20, 21]. Juxtaposing Cdh2^{+} cells with Cdh2^{-} cells induces formation of cortical actin belts (Figure 2B) reminiscent of those formed at the boundaries within germ-layer explant aggregates, along *Drosophila* embryonic compartment boundaries, at zebrafish rhombomere boundaries and in zebrafish somites, indicating that differential Cdh2 levels can drive tissue boundary formation within the paraxial mesoderm [5, 8, 16, 22]. The Cdh2^{+}/Cdh2^{-} boundary cells are also polarized with columnar cell shape, basal nucleus, and apical centrosomes, as is observed along somite boundaries (Figure 2C) [16].

Unlike the boundaries observed in in vitro cell-sorting experiments, at rhombomeres, and in *Drosophila* embryonic compartments, somite boundaries contain FN matrix. This matrix is necessary for somite morphogenesis as nascent boundaries quickly dissipate if the ECM is not properly established [23, 24]. Moreover, ectopic ECM assembly can be induced by precocious mis-expression of *cdh2* in the *Xenopus* gastrula [6]. Having found that differential Cdh2 levels induce other aspects of tissue boundary formation within the paraxial mesoderm, we sought to determine whether they also promote boundary ECM assembly.

Using the conformation-specific monoclonal antibody SNAKA51, we detect the active conformation of Itgα5 at Cdh2^{+}/Cdh2^{-} clonal interfaces, indicating that differential Cdh2 levels stimulate Itgα5 activity (Figure 2D) [17, 25]. Consistent with increased Itgα5 activity, Cdh2^{+}/Cdh2^{-} interfaces contain robust FN matrix (Figures 2D–2F). We created an ImageJ macro to quantify the percentage of the clone boundary that formed FN matrix (Figures 2F and 2G). This ECM assembly is present whether Cdh2 is depleted from either the donor or the host, showing that it is a specific result of differential Cdh2 levels at the clonal boundary (Figures 2E and 2G). These data indicate that juxtaposition of cells with sharp differences in Cdh2 levels is sufficient to induce boundary formation and ECM assembly.

Cdh2 and Itgα5 Function Redundantly to Promote Tissue Boundary Formation

The sharp juxtaposition of stable Cdh2 levels coupled with the boundary forming activity of differential Cdh2 expression implicates Cdh2 as an effector of somite morphogenesis. However, *cdh2*$^{-/-}$ embryos do not display obvious somite boundary defects, as observed via differential interference contrast (DIC) (Figures 3A, 3B, and S2) or via FN immunolocalization (Figures 3C and S2) [20, 21]. The interplay between cell-cell and cell-ECM interactions revealed by our mosaic experiments provides a possible explanation for this lack of boundary defects in *cdh2*$^{-/-}$ embryos. Differential *itgα5* expression, like differential *cdh2* expression, drives ECM assembly at mosaic interfaces [19]. This similarity suggests that Cdh2 and Itgα5 act together to promote somite morphogenesis. Consistent with this model, co-depletion of *cdh2* and *itgα5* results in a complete loss of tissue boundaries within the paraxial mesoderm. *MZitgα5*$^{-/-}$; *cdh2*^{mo} embryos form neither morphological somite boundaries (Figures 3A and 3B) nor somite boundary FN matrix (Figure 3C). Additionally, the dorsolateral ECM in these embryos is much sparser and poorly cross-linked compared with the dense matrix formed on the paraxial mesoderm in wild-type embryos (Figures 3C and 4A). Together, these data demonstrate that Cdh2 promotes FN matrix formation along paraxial mesoderm tissue boundaries and that it does so in parallel with Itgα5.

This functional redundancy between cell-cell and cell-ECM adhesion contributes to a growing body of data suggesting that these two seemingly disparate processes cooperate to effect morphogenesis. Itgα5 interactions can mediate cell sorting much as cadherins classically do, while cadherin adhesion regulates the mechanics of cell-FN interactions necessary for ECM assembly [6, 26–28]. Notably, there is no evidence that Cdh2 directly interacts with FN, rendering it highly unlikely that Cdh2 and Itgα5 directly compensate for one another. It is more likely that Cdh2 stimulates ECM assembly by elevating the activity of both Itgα5 (Figure 3) and another FN receptor, ItgαV, which partially compensates for loss of Itgα5 during somitogenesis [29, 30]. This epistatic relationship parallels that between *ephrinB2a* and *itgα5*. Loss of *ephrinB2a* alone has no somite phenotype, but knockdown of *ephrinB2a* enhances the *itgα5*$^{-/-}$ somite phenotype [24]. In addition, reverse signaling by *ephrinB2a* is sufficient to activate Itgα5 and induce tissue boundary formation in the paraxial mesoderm [16, 19, 31, 32]. Thus, due to genetic redundancy, synergistic loss-of-function phenotypes in *cdh2*^{mo}*;MZitgα5*$^{-/-}$ and *ephrinB2a*^{mo}*;itgα5*$^{-/-}$ embryos are consistent with Cdh2 and ephrinB2a promoting Itgα5 activity.

Cdh2 and Itgα5 Redundantly Inhibit Mesenchymal ECM Assembly

Examination of *MZitgα5*$^{-/-}$*;cdh2*^{mo} embryos reveals another functional redundancy between Cdh2 and Itgα5. These embryos exhibit a dramatic increase in ectopic FN matrix throughout the mesenchyme of the paraxial mesoderm (Figures 3D and 4A). Itgα5 is known to have an inhibitory role on mesenchymal ECM assembly, but *MZitgα5*$^{-/-}$ embryos do not exhibit any detectable ectopic mesenchymal ECM [19]. By contrast, *cdh2*$^{-/-}$ embryos exhibit an increase in mesenchymal fibronectin in the paraxial mesoderm. As with the stimulatory function, the inhibitory functions of Cdh2 on ECM formation are evident in the Cdh2 genetic mosaics. Cdh2-deficient cells, either host or donor, exhibit mesenchymal FN matrix, while their Cdh2^{+} neighbors do not (Figures 4B and 4C). Further, FN matrix

permeates both donors and hosts of Cdh2-deficient clones in Cdh2-deficient hosts (Figures 2E and 2G, yellow). Thus, in addition to stimulating ECM assembly at tissue boundaries, Cdh2 inhibits ectopic ECM assembly within the tissue mesenchyme. While Cdh2 localization is anti-correlated with sites of ECM assembly in the paraxial mesoderm [17], the observation that *cdh2* is necessary for ECM assembly in *MZitgα5*$^{-/-}$ embryos indicates that *cdh2* is actively required for ECM assembly rather than *cdh2* promoting ECM solely via lack of repression of ECM assembly.

Cdh2 Stimulates and Inhibits ECM Assembly

Cdh2 mediates homotypic adhesion through its extracellular domain and binds β-catenin via its intracellular domain. β-catenin also binds α-catenin, which links the adhesion complex to the actin cytoskeleton [33]. Cadherins can mediate different cellular behaviors through β-catenin-dependent and β-catenin-independent mechanisms [34, 35]. For example, β-catenin-dependent canonical Wnt signaling is reduced in *cdh2*$^{-/-}$ mice [36]. In contrast, β-catenin-independent mechanisms are likely mechanical in nature, functioning either by linking the actomyosin cortices on opposing cells or by inducing cytoskeletal rearrangements [37]. This mechanical mechanism for Cdh2 stimulation of FN matrix assembly is supported by in vitro observations that Cdh engagement organizes cell-ECM traction forces to the peripheries of 2D cell clones and that actomyosin-dependent mechanical force is necessary for FN matrix assembly [6, 27, 28].

To test the β-catenin dependence of the functions of Cdh2 in paraxial mesoderm boundary formation, we employ a chimeric construct (Cdh2Δβ-Cat) in which zebrafish Cdh2 is fused directly to α-catenin with the β-catenin binding domains of both being removed (Figure 4D). Similar constructs have been used by multiple groups in the past and have been shown to successfully recapitulate the adhesive functions of Cdh2 without binding β-catenin [34, 35]. We first test whether β-catenin binding is necessary to mediate the stimulatory role of Cdh2 on ECM assembly by injecting either the Cdh2Δβ-Cat construct or full-length Cdh2 into *cdh2*-deficient donor embryos, and transplanting the resulting cells into *cdh2*-deficient hosts. Both constructs significantly increase the percentage of FN coverage at the clonal boundary (Figure 4E), indicating that β-catenin binding is not necessary for the stimulatory role of Cdh2. To investigate whether this stimulatory role is mediated by increasing cytoskeletal and tissue stiffness, we increase actomyosin contractility via expression of a constitutively active myosin regulatory light chain (caMRLC) in Cdh2-deficient mosaics [17, 38, 39]. Indeed, caMRLC rescues FN matrix assembly along the clone boundaries (Figure 4E).

We then test whether β-catenin binding is necessary to mediate the inhibitory role of Cdh2 on ECM assembly by expressing either the Cdh2Δβ-Cat construct or full-length Cdh2 in *cdh2*-deficient donor embryos and transplanting the resulting cells into cdh2-positive hosts. Full-length Cdh2 is sufficient to inhibit FN matrix assembly, but the Cdh2Δβ-Cat construct is insufficient (Figure 4E). Thus, in order to mediate its inhibitory role on ECM assembly, Cdh2 must bind β-catenin.

Model: A Sawtooth Pattern of Stable Cdh2 Adhesions Affects the Spacing of Morphological Somite Boundaries

The functions of Cdh2 can be integrated with a model suggested by the sawtooth pattern of stable Cdh2 adhesions. Within the mesenchymal core of the somite, cells are surrounded by neighbors with similar levels of stable Cdh2, and the inhibitory role predominates and prevents FN matrix assembly. We recently found that Cdh2 forms a physical complex with Itgα5 that helps repress Itgα5 activation. This complex is present in the presomitic mesoderm but is absent from the somite border [17]. The fact that boundary ECM is lost in embryos lacking both Cdh2 and Itgα5 indicate that it is not the mere absence of Cdh2 repression that stimulates boundary ECM assembly along the somite boundary. The observation that the Cdh2Δβ-Cat construct rescues the stimulatory but not inhibitory role of Cdh2 on ECM formation also suggests that Cdh2 regulates ECM assembly bimodally via two distinct mechanisms. Our data indicate that cells encounter neighbors with starkly different Cdh2 levels at somite boundaries and suggest that Cdh2 promotes boundary formation and ECM assembly by increasing tissue stiffness within the posterior of each somite.

Prior studies have shown that Eph/ephrin signaling leads to somite boundary formation, activation of Itgα5 and ECM assembly [40]. *ephA4* is expressed in the anterior of each somite while *ephrinB2A* is expressed in the posterior of each somite. EphrinB2A protein overlaps with stable Cdh2 but this segmental pattern of ephrinB2a does not require *cdh2* (Figure S3). EphrinB2a only exhibits a sharp border along the posterior of the somite, and this colocalizes with the highest density of EphA4 phosphorylation and the somite boundary [19]. Notably, EphA4 activation along the somite boundary does not require Cdh2 (Figure S3).

It has never been clear why boundaries do not form along the interface of Eph/ephrin expression in the mesenchymal core of the somite. However, our data indicate that within the presumptive core of the forming somite, Eph/ephrin interaction domains fall within the Cdh2 gradient, where Cdh2 mediates its inhibitory role to prevent matrix formation (Figure 4F). Indeed, *cdh2*$^{-/-}$ embryos exhibit increased EphA4 activation (Figure S3) and FN matrix assembly within the somite mesenchyme [17]. Even more dramatically, *cdh2*$^{-/-}$ mice exhibit fission of somites into anterior and posterior halves, which is consistent with intrasomitic Eph/ephrin boundary formation being revealed by the loss of *cdh2* [41]. Thus, the sawtooth pattern of Cdh2 and the inhibitory effects of Cdh2 on ECM assembly suppress intrasomitic boundary formation.

The consensus model for somitogenesis, called the clock and wavefront model, centers on transcriptional oscillations that establish the segmental pattern of Eph/ephrin expression presaging somite boundary morphogenesis [42]. In agreement with this model, we found that the sawtooth pattern of stable Cdh2 also requires segmental patterning downstream of *fused somites/tbx6* (Figure S3) [19]. However, a recent report suggested that paraxial mesoderm transplants are mechanically tuned to form spheroids of specific sizes in the absence of segmental patterning [43]. This conclusion is belied by overwhelming genetic evidence indicating that normal somitogenesis requires segmentation clock function and that failure of this mechanism leads to vertebral abnormalities in zebrafish, mice, and humans

[44]. The repression of FN matrix assembly within the paraxial mesoderm mesenchyme that we have reported here and elsewhere suggests that the paraxial mesoderm indeed has an intrinsic bias to make FN matrix its surface [17, 19]. Here, we also find that a sawtooth pattern of Cdh2 stability and differential Cdh2 levels promote somite boundary morphogenesis. Thus, cell-sorting models used to explain spheroid formation parallel the role of Cdh2 in promoting somite boundary morpho-genesis. However, sorting models and cell-sorting experiments demonstrate the importance of surrounding media and cells on cell sorting and spheroid formation [5, 45]. Therefore, while some experimental conditions may allow the paraxial mesoderm to form spheroids in the apparent absence of segmental patterning, the preponderance of evidence supports a model in which the segmentation clock patterns the paraxial mesoderm to harness intrinsic cell-cell and cell-ECM mechanics of the paraxial mesoderm to robustly form regular, bilaterally symmetric somites during normal vertebrate development.

EXPERIMENTAL PROCEDURES

Zebrafish Care and Strains

Zebrafish were maintained in accordance with standard protocols approved by the Yale University IACUC. Wild-type strains used are Tübingen, TLAB, and TLF. The *Itgα5* mutant allele used is *bfe*^{thl30} [23]. The *cdh2* mutant allele used is *pac*^{tm101} [20]. *MZitgα5*$^{-/-}$*;cdh2*^{mo} embryos were created by injecting 50 μM *cdh2*^{mo} [17, 20, 21] into maternal zygotic (*MZ*) *MZitgα5*$^{-/-}$ embryos. FN and SNAKA51 Itgα5 immunohistochemistry were performed as previously described [17, 19].

Cell-Shape Analysis

Cells were manually traced and fit with ellipses as described in the Supplemental Experimental Procedures. Fixed *cdh2-sfGFP-TagRFP* embryos were used for Figures 1C and 1D, and phalloidin-stained embryos were used for Figure 1F.

Cdh2 Timer Quantitative Analysis

Cells of *cdh2-sfGFP-TagRFP* embryos were manually traced and fit with an ellipse in ImageJ. The mean red pixel intensity was calculated by using the sfGFP image to mask the TagRFP image, drawing a series of rectangles 2.2 μm wide and spanning the somite medial to lateral, and measuring the mean red pixel intensity within these rectangles (see Supplemental Experimental Procedures).

Mosaic Analysis

Heterochronic transplants were performed as previously described [19]. *cdh2* depletion was achieved by injecting 50 μM *cdh2*^{mo} into 1-cell stage blastomeres. Full-length zebrafish Cdh2 fused with mRFP at the C terminus was injected at 200 ng/μl for the stimulatory role rescue experiments and 50 ng/μl for the inhibitory role rescue experiments. The Cdh2Δβ-Cat construct was generated by fusing base pairs 1–2463 from zebrafish *cdh2* to base pairs 604–2724 of zebrafish *ctnna1* and was injected at 200 ng/μl. caMRLC-emGFP was injected at 75 ng/μl, GFP-Centrin was injected at 5 ng/μl, mem-RFP was injected at 50 ng/μl, and DAPI was used at 5 μg/μl. Percentage of FN coverage was quantified by blurring both the

rhodamine signal and FN immunostain signal and converting both into binary masks, tracing the binary mask of the rhodamine signal, and measuring what percentage of the trace colocalized with signal from the binary FN mask (see Supplemental Experimental Procedures).

Supplementary Material

Refer to Web version on PubMed Central for supplementary material.

ACKNOWLEDGMENTS

We thank Joe Wolenski for microscopy support and Dipjyoti Das for comments on the manuscript and assistance with data analysis. Funding was provided by NSF grant IOS-1051839 and NIH grant R01GM107385A-01A1 to S.A.H. and NIH Predoctoral Training Grant T32GM007223 to P.M.

REFERENCES

1. Steinberg MS, Gilbert SF. Townes and Holtfreter (1955): directed movements and selective adhesion of embryonic amphibian cells. J. Exp. Zoolog. A Comp. Exp. Biol. 2004; 301:701–706.
2. Nose A, Nagafuchi A, Takeichi M. Expressed recombinant cadherins mediate cell sorting in model systems. Cell. 1988; 54:993–1001. [PubMed: 3416359]
3. Duguay D, Foty RA, Steinberg MS. Cadherin-mediated cell adhesion and tissue segregation: qualitative and quantitative determinants. Dev. Biol. 2003; 253:309–323. [PubMed: 12645933]
4. Foty RA, Steinberg MS. The differential adhesion hypothesis: a direct evaluation. Dev. Biol. 2005; 278:255–263. [PubMed: 15649477]
5. Krieg M, Arboleda-Estudillo Y, Puech PH, Käfer J, Graner F, Müller DJ, Heisenberg CP. Tensile forces govern germ-layer organization in zebrafish. Nat. Cell Biol. 2008; 10:429–436. [PubMed: 18364700]
6. Dzamba BJ, Jakab KR, Marsden M, Schwartz MA, DeSimone DW. Cadherin adhesion, tissue tension, and noncanonical Wnt signaling regulate fibronectin matrix organization. Dev. Cell. 2009; 16:421–432. [PubMed: 19289087]
7. Landsberg KP, Farhadifar R, Ranft J, Umetsu D, Widmann TJ, Bittig T, Said A, Jülicher F, Dahmann C. Increased cell bond tension governs cell sorting at the Drosophila anteroposterior compartment boundary. Curr. Biol. 2009; 19:1950–1955. [PubMed: 19879142]
8. Monier B, Pelissier-Monier A, Brand AH, Sanson B. An actomyosin-based barrier inhibits cell mixing at compartmental boundaries in Drosophila embryos. Nat. Cell Biol. 2010; 12:60–65. [PubMed: 19966783]
9. Brodland GW, Conte V, Cranston PG, Veldhuis J, Narasimhan S, Hutson MS, Jacinto A, Ulrich F, Baum B, Miodownik M. Video force microscopy reveals the mechanics of ventral furrow invagination in Drosophila. Proc. Natl. Acad. Sci. USA. 2010; 107:22111–22116. [PubMed: 21127270]
10. Manning ML, Foty RA, Steinberg MS, Schoetz EM. Coaction of intercellular adhesion and cortical tension specifies tissue surface tension. Proc. Natl. Acad. Sci. USA. 2010; 107:12517–12522. [PubMed: 20616053]
11. Maître JL, Heisenberg CP. Three functions of cadherins in cell adhesion. Curr. Biol. 2013; 23:R626–R633. [PubMed: 23885883]
12. Cavey M, Rauzi M, Lenne PF, Lecuit T. A two-tiered mechanism for stabilization and immobilization of E-cadherin. Nature. 2008; 453:751–756. [PubMed: 18480755]
13. Fagotto F, Rohani N, Touret AS, Li R. A molecular base for cell sorting at embryonic boundaries: contact inhibition of cadherin adhesion by ephrin/ Eph-dependent contractility. Dev. Cell. 2013; 27:72–87. [PubMed: 24094740]
14. Revenu C, Streichan S, Donà E, Lecaudey V, Hufnagel L, Gilmour D. Quantitative cell polarity imaging defines leader-to-follower transitions during collective migration and the key role of

microtubule-dependent adherens junction formation. Development. 2014; 141:1282–1291. [PubMed: 24595289]

15. Crawford BD, Henry CA, Clason TA, Becker AL, Hille MB. Activity and distribution of paxillin, focal adhesion kinase, and cadherin indicate cooperative roles during zebrafish morphogenesis. Mol. Biol. Cell. 2003; 14:3065–3081. [PubMed: 12925747]
16. Barrios A, Poole RJ, Durbin L, Brennan C, Holder N, Wilson SW. Eph/Ephrin signaling regulates the mesenchymal-to-epithelial transition of the paraxial mesoderm during somite morphogenesis. Curr. Biol. 2003; 13:1571–1582. [PubMed: 13678588]
17. Jülich D, Cobb G, Melo AM, McMillen P, Lawton AK, Mochrie SGJ, Rhoades E, Holley SA. Cross-scale Integrin regulation organizes ECM and tissue topology. Dev. Cell. 2015; 34:33–44. [PubMed: 26096733]
18. Durbin L, Sordino P, Barrios A, Gering M, Thisse C, Thisse B, Brennan C, Green A, Wilson S, Holder N. Anteroposterior patterning is required within segments for somite boundary formation in developing zebrafish. Development. 2000; 127:1703–1713. [PubMed: 10725246]
19. Jülich D, Mould AP, Koper E, Holley SA. Control of extra-cellular matrix assembly along tissue boundaries via Integrin and Eph/Ephrin signaling. Development. 2009; 136:2913–2921. [PubMed: 19641014]
20. Lele Z, Folchert A, Concha M, Rauch GJ, Geisler R, Rosa F, Wilson SW, Hammerschmidt M, Bally-Cuif L. parachute/ n-cadherin is required for morphogenesis and maintained integrity of the zebrafish neural tube. Development. 2002; 129:3281–3294. [PubMed: 12091300]
21. Warga RM, Kane DA. A role for N-cadherin in mesodermal morphogenesis during gastrulation. Dev. Biol. 2007; 310:211–225. [PubMed: 17826762]
22. Calzolari S, Terriente J, Pujades C. Cell segregation in the vertebrate hindbrain relies on actomyosin cables located at the interhombomeric boundaries. EMBO J. 2014; 33:686–701. [PubMed: 24569501]
23. Jülich D, Geisler R, Holley SA, Holley SA, Tübingen 2000 Screen Consortium. Integrinalpha5 and delta/notch signaling have complementary spatiotemporal requirements during zebrafish somitogenesis. Dev. Cell. 2005; 8:575–586. [PubMed: 15809039]
24. Koshida S, Kishimoto Y, Ustumi H, Shimizu T, Furutani-Seiki M, Kondoh H, Takada S. Integrinalpha5-dependent fibronectin accumulation for maintenance of somite boundaries in zebrafish embryos. Dev. Cell. 2005; 8:587–598. [PubMed: 15809040]
25. Clark K, Pankov R, Travis MA, Askari JA, Mould AP, Craig SE, Newham P, Yamada KM, Humphries MJ. A specific alpha5beta1-integrin conformation promotes directional integrin translocation and fibronectin matrix formation. J. Cell Sci. 2005; 118:291–300. [PubMed: 15615773]
26. Caicedo-Carvajal CE, Shinbrot T, Foty RA. Alpha5beta1 integrin-fibronectin interactions specify liquid to solid phase transition of 3D cellular aggregates. PLoS ONE. 2010; 5:e11830. [PubMed: 20686611]
27. Mertz AF, Che Y, Banerjee S, Goldstein JM, Rosowski KA, Revilla SF, Niessen CM, Marchetti MC, Dufresne ER, Horsley V. Cadherin-based intercellular adhesions organize epithelial cell-matrix traction forces. Proc. Natl. Acad. Sci. USA. 2013; 110:842–847. [PubMed: 23277553]
28. Zhong C, Chrzanowska-Wodnicka M, Brown J, Shaub A, Belkin AM, Burridge K. Rho-mediated contractility exposes a cryptic site in fibronectin and induces fibronectin matrix assembly. J. Cell Biol. 1998; 141:539–551. [PubMed: 9548730]
29. Dray N, Lawton A, Nandi A, Jülich D, Emonet T, Holley SA. Cell-fibronectin interactions propel vertebrate trunk elongation via tissue mechanics. Curr. Biol. 2013; 23:1335–1341. [PubMed: 23810535]
30. Yang JT, Bader BL, Kreidberg JA, Ullman-Culleré M, Trevithick JE, Hynes RO. Overlapping and independent functions of fibronectin receptor integrins in early mesodermal development. Dev. Biol. 1999; 215:264–277. [PubMed: 10545236]
31. Durbin L, Brennan C, Shiomi K, Cooke J, Barrios A, Shanmugalingam S, Guthrie B, Lindberg R, Holder N. Eph signaling is required for segmentation and differentiation of the somites. Genes Dev. 1998; 12:3096–3109. [PubMed: 9765210]

32. Watanabe T, Sato Y, Saito D, Tadokoro R, Takahashi Y. EphrinB2 coordinates the formation of a morphological boundary and cell epithelialization during somite segmentation. Proc. Natl. Acad. Sci. USA. 2009; 106:7467–7472. [PubMed: 19380726]
33. Buckley CD, Tan J, Anderson KL, Hanein D, Volkmann N, Weis WI, Nelson WJ, Dunn AR. Cell adhesion. The minimal cadherin-catenin complex binds to actin filaments under force. Science. 2014; 346:1254211. [PubMed: 25359979]
34. Gottardi CJ, Wong E, Gumbiner BM. E-cadherin suppresses cellular transformation by inhibiting beta-catenin signaling in an adhesion-independent manner. J. Cell Biol. 2001; 153:1049–1060. [PubMed: 11381089]
35. Nagafuchi A, Ishihara S, Tsukita S. The roles of catenins in the cadherin-mediated cell adhesion: functional analysis of E-cadherin-alpha catenin fusion molecules. J. Cell Biol. 1994; 127:235–245. [PubMed: 7929566]
36. Howard S, Deroo T, Fujita Y, Itasaki N. A positive role of cadherin in Wnt/b-catenin signalling during epithelial-mesenchymal transition. PLoS ONE. 2011; 6:e23899. [PubMed: 21909376]
37. Maître JL, Berthoumieux H, Krens SF, Salbreux G, Jülicher F, Paluch E, Heisenberg CP. Adhesion functions in cell sorting by mechanically coupling the cortices of adhering cells. Science. 2012; 338:253–256. [PubMed: 22923438]
38. Iwasaki T, Murata-Hori M, Ishitobi S, Hosoya H. Diphosphorylated MRLC is required for organization of stress fibers in interphase cells and the contractile ring in dividing cells. Cell Struct. Funct. 2001; 26:677–683. [PubMed: 11942626]
39. Norden C, Young S, Link BA, Harris WA. Actomyosin is the main driver of interkinetic nuclear migration in the retina. Cell. 2009; 138:1195–1208. [PubMed: 19766571]
40. McMillen P, Holley SA. The tissue mechanics of vertebrate body elongation and segmentation. Curr. Opin. Genet. Dev. 2015; 32:106–111. [PubMed: 25796079]
41. Horikawa K, Radice G, Takeichi M, Chisaka O. Adhesive subdivisions intrinsic to the epithelial somites. Dev. Biol. 1999; 215:182–189. [PubMed: 10545229]
42. Oates AC, Morelli LG, Ares S. Patterning embryos with oscillations: structure, function and dynamics of the vertebrate segmentation clock. Development. 2012; 139:625–639. [PubMed: 22274695]
43. Dias AS, de Almeida I, Belmonte JM, Glazier JA, Stern CD. Somites without a clock. Science. 2014; 343:791–795. [PubMed: 24407478]
44. Pourquié O. Vertebrate segmentation: from cyclic gene networks to scoliosis. Cell. 2011; 145:650–663. [PubMed: 21620133]
45. Wayne Brodland G, Chen HH. The mechanics of cell sorting and envelopment. J. Biomech. 2000; 33:845–851. [PubMed: 10831759]

Highlights

- A gradient of cadherin 2 stability is observed in each somite
- Cadherin 2 promotes epithelialization of the posterior somite
- Differential cadherin 2 levels induce integrin α5 activation and border formation
- Cadherin 2 stimulates boundary ECM assembly by increasing tissue stiffness

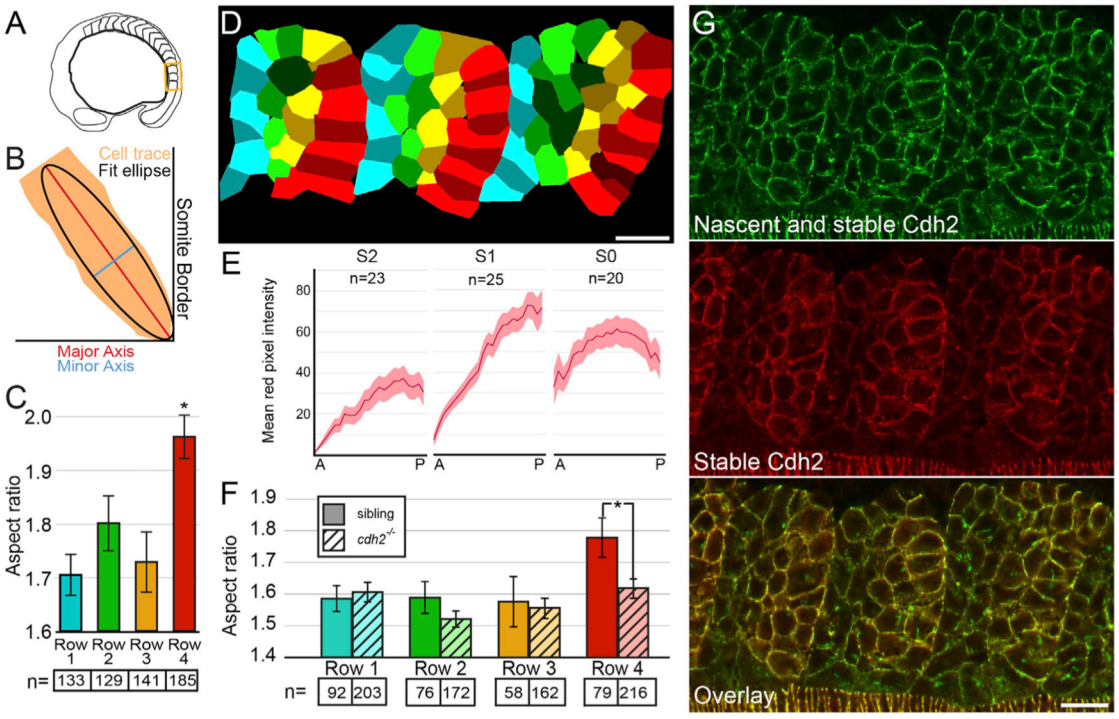

Figure 1. Cell-Shape Changes Correlate with Graded Stable Cdh2 Adhesions along Posterior Somite Border Cells

(A) A schematic of the region of the embryo containing the most recently formed somites imaged in (D) and (G).

(B) The aspect ratio of cell traces was determined by dividing the major axis length by the minor axis length of a fit ellipse.

(C and D) Posterior somite boundary cells (row 4, red) exhibit an increased aspect ratio compared with row 1 cells ($p < 0.00001$, t test).

(E and G) Somites exhibit graded levels of stable Cdh2 (red) adhesion increasing from anterior to posterior.

(F) The aspect ratio of posterior somite boundary cells is reduced in *cdh2*$^{-/-}$ embryos ($p < 0.01$, t test).

n, number of cells for (C) and (F); n, number of somites for (E). Mean values indicated ± SEM. Scale bars, 20 μm. See also Figure S1.

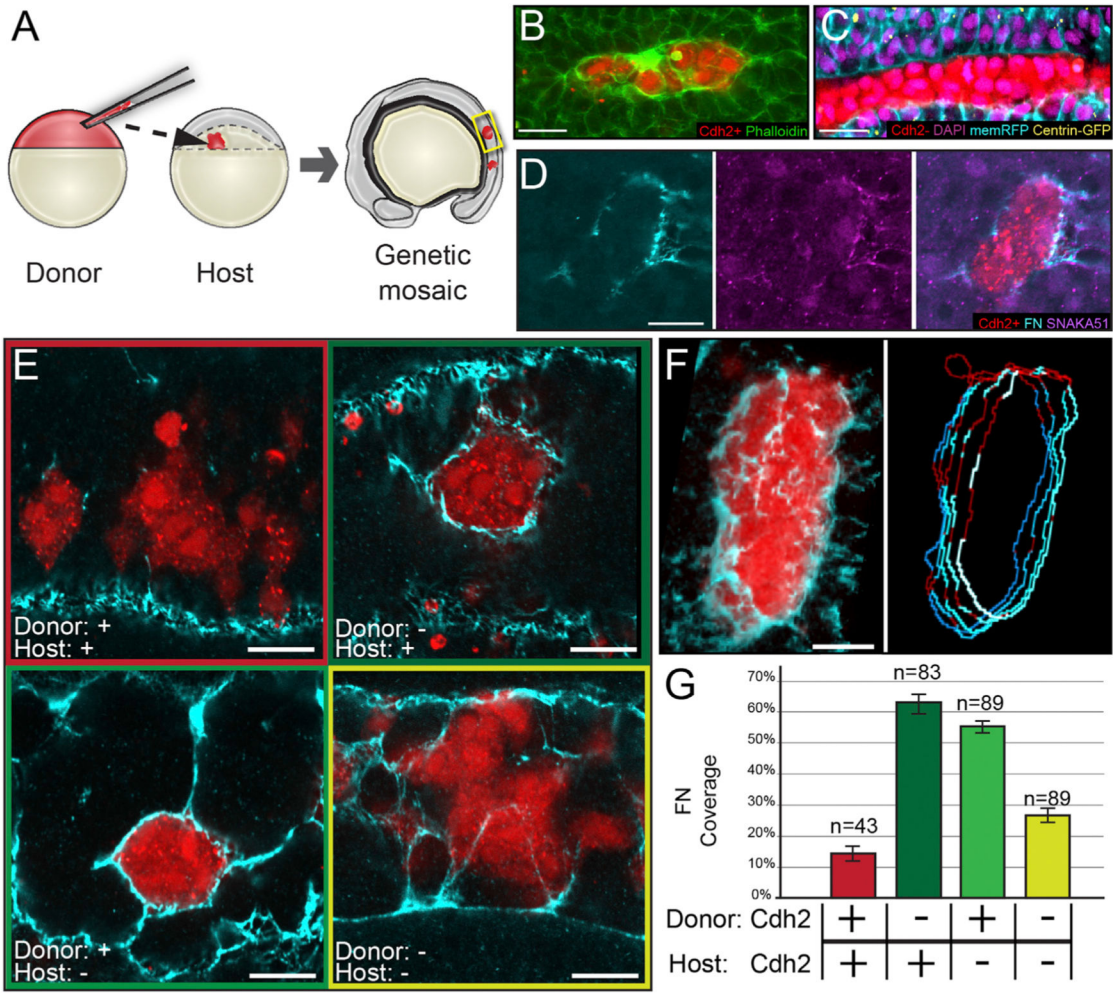

Figure 2. Differential *cdh2* Expression Stimulates Tissue Boundary Formation

(A) Genetic mosaics were generated by transplanting blastomeres from early blastula-stage donors labeled with fluorescent dextran (rhodamine or Alexa Fluor 647) into later blastula-stage hosts.

(B) Clones were analyzed for F-actin localization via phalloidin staining. 17 of 27 clones exhibited strong cortical actin.

(C) Cdh2-expressing cells polarize toward boundaries with Cdh2-deficient cells. Ten of 12 clones exhibit columnar cell shape, basal nuclei, and apical centrosomes.

(D) Clones were analyzed for Itgα5 activation using the SNAKA51 antibody and FN matrix assembly. Nine of nine clones displayed activated Itgα5 and FN matrix.

(E) Robust FN matrix forms at boundaries between Cdh2-expressing and Cdh2-deficient cells.

(F and G) The percentage of FN coverage of the rhodamine-labeled clones was quantified in multiple z-slices using an ImageJ macro (see Supplemental Experimental Procedures). Pixels positive for FN are blue; pixels negative for FN are red. n, the number of clones examined.

Scale bars, 20 μm. See also Figure S2.

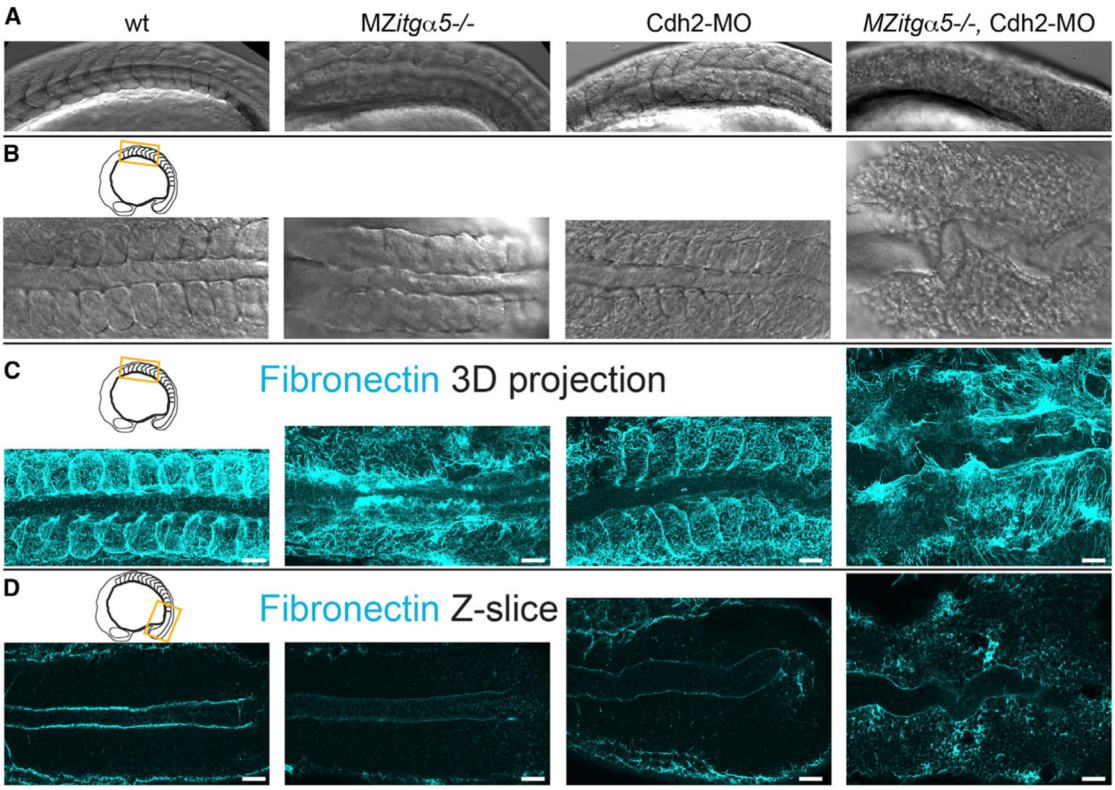

Figure 3. Coordinated Regulation of ECM Assembly by Cdh2 and Itgα5

(A and B) Lateral (A) and dorsal (B) views of the anterior paraxial mesoderm in 10- to 12-somite-stage embryos showing loss of somite borders and de-adhesion of cells in *MZitgα5*$^{-/-}$;*cdh2*^{mo} embryos (n = 8).

(C) 3D dorsal projection of anterior paraxial mesoderm FN immunolocalization z stacks showing loss of dorsolateral FN in *MZitgα5*$^{-/-}$;*cdh2*^{mo} embryos.

(D) Single dorsal z-slices of FN immunolocalization of posterior paraxial mesoderm showing globular FN in *cdh2*^{mo} embryos and diffuse ectopic FN in *MZitgα5*$^{-/-}$;*cdh2*^{mo} embryos.

Scale bars, 40 μm.

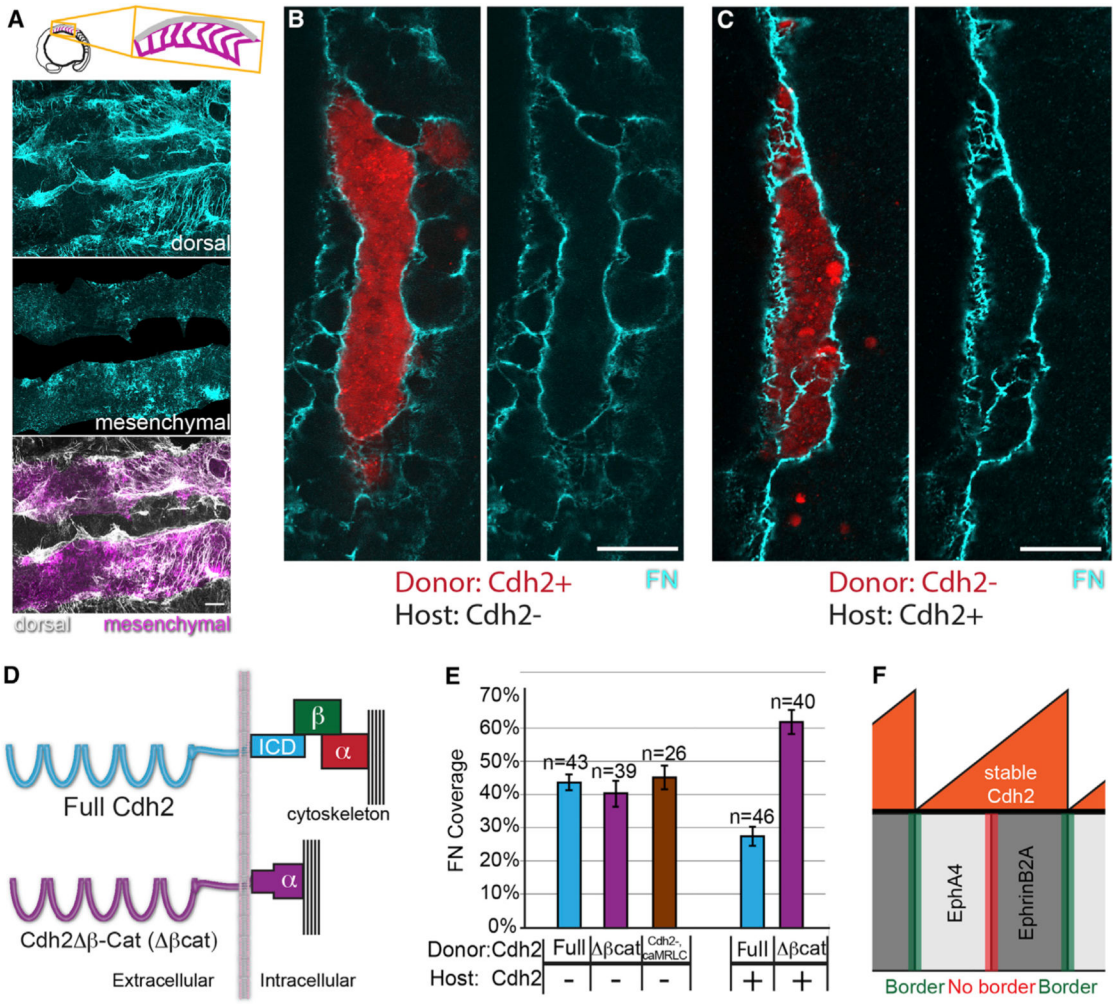

Figure 4. Cdh2 Bimodally Regulates ECM Assembly through Distinct Molecular Mechanisms

(A) *MZitgα5*$^{-/-}$*;cdh2*^{mo} embryos exhibit decreased dorsal ECM assembly and increased ectopic mesenchymal ECM.

(B and C) In mosaic embryos, mesenchymal ECM forms in either Cdh2^{-} hosts (B) or donor clones (C), but not among Cdh2^{+} neighboring cells.

(D) Schematic of the Cdh2Δβ-Cat (Δβcat) construct in which Cdh2 is fused directly to α-catenin, thus mediating adhesion without binding β-catenin.

(E) Δβcat stimulates FN matrix assembly to the same extent as full-length Cdh2 ($p > 0.25$) but does not inhibit FN matrix assembly ($p < 0.0001$). caMRLC also stimulates FN matrix assembly ($p < 0.0001$) to the same extent as full-length Cdh2 and Cdh2Δβ-Cat ($p > 0.25$). n, number of clones examined. Mean values indicated ± SEM. Scale bars, 20 μm. p values were determined by t test.

(F) A model schematic showing graded stable Cdh2 levels inhibiting boundary formation at Eph/ephrin interfaces within somites while differential levels of stable Cdh2 promote boundary formation at Eph/ephrin interfaces between somites.

See also Figure S3.